

Published in final edited form as:

*Nitric Oxide*. 2014 May 30; 39: 46–50. doi:10.1016/j.niox.2014.04.001.

## Crystallographic Characterization of the Nitric Oxide Derivative of *R*-State Human Hemoglobin

Jun Yi<sup>a,b</sup>, Alexei S. Soares<sup>c</sup>, and George B. Richter-Addo<sup>\*,a</sup>

<sup>a</sup>Department of Chemistry and Biochemistry, University of Oklahoma, 101 Stephenson Parkway, Norman, Oklahoma. U.S.A., 73019

<sup>b</sup>Department of Biological Engineering, Nanjing University of Science and Technology, Nanjing, China 210094

<sup>c</sup>Macromolecular Crystallography Research Resource, National Synchrotron Light Source, Brookhaven National Laboratory, Upton, NY 11973. USA

### Abstract

Nitric oxide (NO) is a signaling agent that is biosynthesized *in vivo*. NO binds to the heme center in human hemoglobin (Hb) to form the HbNO adduct. This reaction of NO with Hb has been studied for many decades. Of continued interest has been the effect that the bound NO ligand has on the geometrical parameters of the resulting heme-NO active site. Although the crystal structure of a *T*-state human HbNO complex has been published previously, that of the high affinity *R*-state HbNO derivative has not been reported to date. We have crystallized and solved the three-dimensional X-ray structure of *R*-state human HbNO to 1.90 Å resolution. The differences in the FeNO bond parameters and H-bonding patterns between the  $\alpha$  and  $\beta$  subunits contribute to understanding of the observed enhanced stability of the  $\alpha$ (FeNO) moieties relative to the  $\beta$ (FeNO) moieties in human *R*-state HbNO.

### Keywords

Hemoglobin; Iron; Nitric Oxide; X-ray; Nitrosyl

### Introduction

Nitric oxide (NO) is biosynthesized in mammals from *L*-arginine by the heme enzyme NO synthase [1]. The NO that is generated serves as a biological signaling agent that binds to the

© 2014 Elsevier Inc. All rights reserved

Correspondence to: Jun Yi.

\*grichteraddo@ou.edu.

**Publisher's Disclaimer:** This is a PDF file of an unedited manuscript that has been accepted for publication. As a service to our customers we are providing this early version of the manuscript. The manuscript will undergo copyediting, typesetting, and review of the resulting proof before it is published in its final citable form. Please note that during the production process errors may be discovered which could affect the content, and all legal disclaimers that apply to the journal pertain.

**Supporting Information** Figure showing a superposition of the  $\alpha\beta$ 2 interfaces of selected Hb structures of known quaternary conformations (Fig. S1).

ferrous heme of the enzyme soluble guanylyl cyclase (sGC) resulting in the cleavage of the *trans* bond between the heme Fe and the proximal His ligand of sGC [2, 3]. This important Fe–N(His) bond cleavage correlates with observed vasodilation and regulation of blood pressure [3]. NO can also be generated by other metalloproteins using ubiquitous inorganic nitrite as a reagent (e.g., under hypoxic conditions) [4], although the relative contribution of this latter NO generation pathway is still being debated.

NO binds to human hemoglobin (Hb) *in vivo* to form the HbNO adduct [5]. This adduct can form under normal physiological conditions, although its steady state concentrations are normally very low (e.g., estimated in some cases at less than 0.1% of the total Hb) [6]. Yonetani and coworkers have shown that Hb can effectively react with low concentrations of NO via binding to the  $\alpha$ hemes [7]. Importantly, they also demonstrated that the resulting  $\alpha(\text{FeNO})_2\beta(\text{Fe})_2$  derivative “becomes a cooperative low affinity O<sub>2</sub> carrier that can deliver O<sub>2</sub> to tissues as efficiently as native Hb under physiological conditions”, although it only carries two molecules of O<sub>2</sub> instead of four [7].

Low-temperature electron paramagnetic resonance (EPR) studies of human tetrameric HbNO at pH 7.3 suggested six-coordination at the Fe sites, i.e., both NO and the proximal His remain coordinated to the heme [8], consistent with an earlier single-crystal EPR study [9]. The data obtained at low pH, however, reveals a shift towards five-coordination where the proximal Fe–His bond is either cleaved or severely weakened [8]. Not surprisingly, acidification has been employed for the removal of heme from His-ligated heme proteins such as Hb and Mb [10, 11]. The *R*-state to *T*-state transition for human HbNO was achieved upon addition of IHP, accompanied by a likely switch from six-coordination of heme Fe to five-coordination for about half of the hemes [12, 13].

Chan et al. prepared single crystals of *T*-state human HbNO and determined its structure [14]. They observed a cleavage of the proximal Fe–His bond in the  $\alpha$ subunit (to yield five-coordinate heme nitrosyl) whereas this proximal Fe–His bond was retained in the  $\beta$ subunit.

We are interested in examining the active site differences between the  $\alpha$  and  $\beta$  subunits of the “high affinity” *R*-state of human Hb in its interactions with various nitrogen oxide ligands. We were surprised to find that despite the physiological relevance of *R*-state HbNO, there was no reported three-dimensional crystal structure of this *R*-state complex. In this article, we report the preparation of crystalline *R*-state HbNO and its crystal structure at 1.90 Å resolution. We show that both hemes remain six-coordinate but with active-site conformational differences of the FeNO moieties in the  $\alpha$  and  $\beta$  subunits.

## Materials and Methods

### Complex formation

Diamond-shaped crystals of ferric *R*-state Hb(ONO) [15] were transferred into 50  $\mu\text{L}$  of degassed 3.2 M Na/K phosphate buffer at pH 6.8 containing 16% glycerol as a cryo-solution. A few grains of solid sodium dithionite were added to this solution and left to stand for 5 min. The resulting bright red crystals were harvested using cryoloops and flash-frozen in liquid nitrogen prior to data collection.

## X-ray data collection and processing

X-ray diffraction data were collected at 100 K at the National Synchrotron Light Source (NSLS) beamline X-29 using an ADSC Quantum-315 CCD detector. 1° oscillation images were collected over a range of 360° with an exposure time of 4 secs/image and a crystal-to-detector distance of 220 mm. Diffraction data were indexed and processed with the d\*TREK program (Macintosh v.99D) [16].

## Structure solution and refinement

The CCP4 *REFMAC5* program [17, 18] was used for the structure solution and refinement. *COOT* [19] was used for visualization and model building/corrections between refinement cycles. The phase information was obtained using the molecular replacement method (*PHASER* [20]) as implemented in CCP4. The 1.25-Å resolution structure of *R*-state human HbCO (PDB accession code 1IRD), with the CO and solvent molecules omitted from the structure, was used as the search model. The initial electron density maps showed positive densities in both the  $\alpha$  and  $\beta$  distal pockets consistent with the presence of diatomic (e.g., NO) rather than triatomic (e.g., the precursor nitrite) ligands. Two NO molecules were modeled into the  $\alpha$  distal pocket (NO at 100%) and  $\beta$  distal pocket (NO at 80%). The Fe–N(O) bond distance and Fe–N–O bond angle parameters were unrestrained throughout the refinement; however, an internal restraint of 1.17(3) Å for d(N–O) was applied to the NO groups consistent with data obtained from high-quality crystal structures of ferrous-NO porphyrins [21, 22]. The complex crystallizes with one  $\alpha/\beta$  dimer in the asymmetric unit.

After completion of the refinement process, the interactive macromolecular structure validation tool *MolPROBITY* (available online from the Richardson Laboratory at Duke University at <http://molprobitry.biochem.duke.edu>) [23] was utilized to assign the final rotamer orientations as Asn, Gln, and His sidechains, and to test for any unusual side-chain contacts. The  $2F_o - F_c$  electron density maps and the  $F_o - F_c$  omit electron density maps were generated using FFT in CCP4, and the  $F_o - F_c$  omit maps were generated using the final model without the NO molecules in the distal pockets. Figures were drawn using *PyMOL* [24] and labels were added using Adobe® Photoshop.

The crystal structure has been deposited with the Protein Data Bank with accession code 4N8T. Selected crystallographic data and refinement statistics are shown in Table 1.

## Results and Discussion

Several methods have been used to prepare the nitrosyl derivative of human hemoglobin, HbNO (reviewed in [5]). Two common preparative methods involve (i) the reaction of Hb with inorganic nitrite in the presence of a reductant, and (ii) the reaction of deoxyHb with NO gas. The Hb-nitrite adduct is a likely intermediate in reaction (i) above, and we previously reported the preparation and X-ray crystal structural determination of ferric *R*-state Hb(ONO) [15] and related nitriheme derivatives [25]. To improve our chances of obtaining the crystal structure of the target *R*-state HbNO complex, we utilized crystalline *R*-state Hb(ONO) for the reaction to generate the nitrosyl derivative. Crystals of Hb(ONO) were prepared as described previously [15] and reacted with sodium dithionite as a

reductant. X-ray diffraction data using synchrotron radiation were collected on the product crystals, and the crystal structure was solved at 1.90-Å resolution.

### Protein Conformation

Safo and coworkers have detailed the crystal structural features that characterize the conformational states of Hb [26]. Examination of the tertiary and quaternary structure of the tetrameric HbNO product, particularly at the critical  $\alpha 1\beta 2$  interface, revealed that this HbNO derivative obtained by reduction of the *R*-state Hb(ONO) precursor retained the *R*-state conformation. Figure S1 shows a C $\alpha$  chain overlay of the  $\alpha 1\beta 2$  interfaces of the HbNO derivative (this work) with *T*-state deoxyHb [27], *R*-state Hb(CO) [28] and aquometHb [29], *R2*-state Hb(CO) [30], and *R3*-state Hb(CO) [31]. An analysis of these structures and the relative positions of their  $\beta 2$  FG corners (Fig. S1) shows that the Hb(NO) obtained in this current work is indeed in the *R*-state conformation.

### Distal FeNO Geometry

The  $2F_o - F_c$  electron density maps, the  $F_o - F_c$  omit electron density maps, and the final model of the heme active site of the *R*-state HbNO derivative obtained in this current work are shown in Figure 1. The NO ligands were modeled at full occupancy in the  $\alpha$  subunit (Fig. 1, top), and best modeled at 80% occupancy in the  $\beta$  subunit (Fig. 1, bottom).

The  $\alpha$  subunit active site (Fig. 1, top) displays an Fe–N–O bond angle of 138° and an Fe–N(O) distance of 1.8 Å that fits well with data obtained from synthetic ferrous nitrosyl porphyrins [5, 21, 22].

The NO ligand is hydrogen-bonded to the distal His58 residue. It appears, at this 1.90-Å resolution, that the H-bonding stabilization of the bound NO ligand involves both N and O atoms, with similar (nitrosyl)N–N(His58) and (nitrosyl)O–N(His58) distances of 2.7 Å and 2.8 Å, respectively.

A fixed water molecule is evident in the electron density map near the exterior surface of the  $\alpha$  subunit, and bridges the distal His58 residue and both heme propionate groups. This water molecule perhaps helps lower the probability of ligand escape from the distal pocket of the  $\alpha$  subunit (see later).

The  $\beta$  subunit active site (Fig. 1, bottom) displays a more acute Fe–N–O bond angle of 125° and a longer Fe–N(O) distance of 2.1 Å. Further, this NO ligand is H-bonded to the distal His63 residue via the nitrosyl N atom with the (nitrosyl)N–N(His63) distance of 2.7 Å. This asymmetrical H-bonding of the NO ligand to the distal His residue in the  $\beta$  subunit is in contrast with that observed for the  $\alpha$  subunit where both the nitrosyl N and O atoms are H-bonded to the distal His residue. Further, we do not observe a fixed water molecule on the distal side of the heme propionate groups. Rather, we observe that the “pointing down” of the heme propionates in the  $\beta$  subunit appears to be stabilized by a fixed water molecule on the proximal side that is H-bonded with one of the propionates.

The differences in the Fe–NO distances and H-bonding patterns of the NO ligands in the  $\alpha$  and  $\beta$  subunits, combined with the propionate orientations and engagement in H-bonding

interactions with crystallographically observed water molecules, suggest an enhanced stabilization of the bound NO in the  $\alpha$  subunit relative to the  $\beta$  subunit. Although not necessarily correlated, we note that these heme site features in the crystal structure of *R*-state HbNO are consistent with the reported observation that “the affinity for NO to  $\alpha$  hemes of Hb is more than 100-fold stronger than that for the  $\beta$  hemes under physiological conditions” [7]. In fact, exposure of human tetrameric deoxyHb to NO under physiological conditions gives a mixture of  $\alpha(\text{FeNO})\alpha(\text{Fe})\beta(\text{Fe})_2$  and  $\alpha(\text{FeNO})_2\beta(\text{Fe})_2$ , in preference to the “ $\alpha(\text{Fe})\beta(\text{FeNO})$ ” analogues [7].

### Proximal heme geometry

The proximal heme geometry in *R*-state HbNO deserves comment. A comparison between the heme sites of ferrous *R*-state HbNO (this work) and ferrous *T*-state HbNO [14] is shown in Figure 2. In *T*-state HbNO, obtained by binding NO to crystals of *T*-state deoxy HbNO, the binding of the NO ligand induced proximal ligand dissociation in the  $\alpha$  subunit but not in the  $\beta$  subunit [14].

In the  $\alpha$  subunit of *T*-state HbNO (Fig. 2, top, gray model), the dissociated proximal His87 ligand ( $\text{Fe}-\text{N}(\text{His87}) = 4.06 \text{ \AA}$ ) is stabilized by H-bonding to a fixed water molecule on the proximal side that in turns H-bonds to Tyr140 and the Val93 backbone [14]. In contrast, the six-coordination is retained in the  $\beta$  subunit of *T*-state HbNO (Fig. 2, bottom) with  $\text{Fe}-\text{N}(\text{His92}) = 2.25 \text{ \AA}$ . A density functional theoretical (DFT) study of the factors responsible for active site differences in *T*-state HbNO revealed that the presence of this fixed water molecule is critical in the stabilization of the cleaved proximal  $\text{Fe}-\text{N}(\text{His87})$  bond [32]. The DFT study also helped explain why the *T*-state  $\beta\text{W37E}$  mutant HbNO derivative retained six-coordination at both  $\alpha$  and  $\beta$  hemes, namely that there was no fixed water molecule in the  $\alpha$  subunit to stabilize, through H-bonding, the cleaved proximal  $\text{Fe}-\text{N}(\text{His87})$  bond [32].

In summary, we have successfully characterized the nitrosyl derivative of human Hb in the *R*-state by X-ray crystallography at 1.90  $\text{\AA}$  resolution. The HbNO product displays six-coordination at the heme sites of both the  $\alpha$  and  $\beta$  subunits. The NO ligand in the  $\alpha$  subunit engages in H-bonding interactions with the distal His residue via both nitrosyl N and O atoms and has normal FeNO bond parameters expected for ferrous nitrosyl porphyrins. The NO ligand in the  $\beta$  subunit displays a long  $\text{Fe}-\text{N}(\text{O})$  bond and a more acute  $\text{Fe}-\text{N}-\text{O}$  bond angle, with H-bonding to the nitrosyl N atom but not the O atom. These structural observations contribute to our understanding of the previously reported stability of the  $\alpha(\text{FeNO})$  unit relative to the  $\beta(\text{FeNO})$  unit in human HbNO.

### Supplementary Material

Refer to Web version on PubMed Central for supplementary material.

### Acknowledgments

We are grateful to the U.S. National Science Foundation (CHE-1213674 to GBRA) and to the National Science Foundation of China (NSFC-21271104 and NSFC-312000555 to JY) for funding for this work. Data for this study were measured at beamline  $\times 29$  of the National Synchrotron Light Source, utilizing the mail-in program. Financial support for NSLS comes principally from the Offices of Biological and Environmental Research and of Basic Energy Sciences of the US Department of Energy, and from the National Center for Research Resources

(P41RR012408) and the National Institute of General Medical Sciences (P41GM103473) of the National Institutes of Health.

## References

- [1]. Alderton WK, Cooper CE, Knowles RG. Nitric Oxide Synthases: Structure, Function and Inhibition. *Biochem. J.* 2001; 357:593–615. [PubMed: 11463332]
- [2]. Marletta MA, Brandish PE, Denninger JW, Kim S, Stone JR, Zhao Y, Deinum G, Schelvis H, Babcock GT. Nitric Oxide Regulation of Guanylate Cyclase Activity. *Faseb J.* 1998; 12:A1332–A1332.
- [3]. Boon EM, Huang SH, Marletta MA. A Molecular Basis for NO Selectivity in Soluble Guanylate Cyclase. *Nat. Chem. Biol.* 2005; 1:53–59. [PubMed: 16407994]
- [4]. Feelisch M, Fernandez BO, Bryan NS, Garcia-Saura MF, Bauer S, Whitlock DR, Ford PC, Janero DR, Rodriguez J, Ashrafiyan H. Tissue Processing of Nitrite in Hypoxia. An Intricate Interplay of Nitric Oxide-Generating and -Scavenging Systems. *J. Biol. Chem.* 2008; 283:33927–33934. [PubMed: 18835812]
- [5]. Cheng, L.; Richter-Addo, GB. Binding and Activation of Nitric Oxide by Metalloporphyrins and Heme. In: Guillard, R.; Smith, K.; Kadish, KM., editors. *The Porphyrin Handbook*. Vol. Vol. 4. Academic Press; New York: 2000. p. 219-291.
- [6]. Angelo M, Hausladen A, Singel DJ, Stamler JS. Interactions of NO with Hemoglobin: From Microbes to Man. *Methods Enzymol.* 2008; 436:131–168. [PubMed: 18237631]
- [7]. Yonetani T, Tsuneshige A, Zhou Y, Chen X. Electron Paramagnetic Resonance and Oxygen Binding Studies of  $\alpha$ -Nitrosyl Hemoglobin. *J. Biol. Chem.* 1998; 273:20323–20333. references therein. [PubMed: 9685383]
- [8]. Ascenzi A, Bocedi A, Fasano M, Gioia M, Marini S, Coletta M. Proton-Linked Subunit Heterogeneity in Ferrous Nitrosylated Human Adult Hemoglobin: An EPR Study. *J. Inorg. Biochem.* 2005; 99:1255–1259. [PubMed: 15833350]
- [9]. Kon H. Paramagnetic Resonance Study of Nitric Oxide Hemoglobin. *J. Biol. Chem.* 1968; 243:4350–4357. [PubMed: 4300550]
- [10]. Yonetani T. Studies on Cytochrome *c* Peroxidase. X. Crystalline Apo- and Reconstituted Holoenzymes. *J. Biol. Chem.* 1967; 242:5008–5013. [PubMed: 6058943]
- [11]. Teale FWJ. Cleavage of the Haem-Protein Link by Acid Methyleneacetone. *Biochim. Biophys. Acta.* 1959; 35:543. [PubMed: 13837237]
- [12]. Maxwell JC, Caughey WS. An Infrared Study of NO Bonding to Heme B and Hemoglobin A. Evidence for Inositol Hexaphosphate Induced Cleavage of Proximal Histidine to Iron Bonds. *Biochemistry.* 1976; 15:388–396. [PubMed: 1247525]
- [13]. Perutz MF, Kilmartin JV, Nagai K, Szabo A, Simon SR. Influence of Globin Structures on the State of the Heme. Ferrous Low Spin Derivatives. *Biochemistry.* 1976; 15:378–387. [PubMed: 1247524]
- [14]. Chan NL, Kavanaugh JS, Rogers PH, Arnone A. Crystallographic Analysis of the Interaction of Nitric Oxide with Quaternary-T Human Hemoglobin. *Biochemistry.* 2004; 43:118–132. [PubMed: 14705937]
- [15]. Yi J, Safo MK, Richter-Addo GB. The Nitrite Anion Binds to Human Hemoglobin via the Uncommon *O*-Nitrito Mode. *Biochemistry.* 2008; 47:8247–8249. [PubMed: 18630930]
- [16]. Pflugrath J. The Finer Things in X-Ray Diffraction Data Collection. *Acta Cryst.* 1999; D55:1718–1725.
- [17]. Bailey S. The CCP4 Suite: Programs for Protein Crystallography. *Acta Cryst.* 1994; D50:760–763.
- [18]. Murshudov GN, Vagin AA, Dodson EJ. Refinement of Macromolecular Structures by the Maximum-Likelihood Method. *Acta Cryst.* 1997; D53:240–255.
- [19]. Emsley P, Lohkamp B, Scott WG, Cowtan K. Features and Development of *COOT*. *Acta Cryst.* 2010; D66:486–501.
- [20]. McCoy AJ, Grosse-Kunstleve RW, Adams PD, Winn MD, Storoni LC, Read RJ. *PHASER* Crystallographic Software. *J. Appl. Cryst.* 2007; 40:658–674. [PubMed: 19461840]

- [21]. Wyllie GRA, Scheidt WR. Solid-State Structures of Metalloporphyrin NO<sub>x</sub> Compounds. *Chem. Rev.* 2002; 102:1067–1089. [PubMed: 11942787]
- [22]. Wyllie GRA, Schultz CE, Scheidt WR. Five- to Six-Coordination in (Nitrosyl)iron(II) Porphyrinates: Effects of Binding the Sixth Ligand. *Inorg. Chem.* 2003; 42:5722–5734. [PubMed: 12950223]
- [23]. Chen VB, Arendall WB, Headd JJ, Keedy DA, Immormino RM, Kapral GJ, Murray LW, Richardson JS, Richardson DC. *MolProbity*: All-atom Structure Validation for Macromolecular Crystallography. *Acta Cryst.* 2010; D66:12–21.
- [24]. DeLano, WL. DeLano Scientific LLC. San Carlos, CA, U.S.A.: 2006. The *PyMOL* Molecular Graphics System.
- [25]. Yi J, Thomas LM, Musayev FN, Safo MK, Richter-Addo GB. Crystallographic Trapping of Heme Loss Intermediates during the Nitrite-Induced Degradation of Human Hemoglobin. *Biochemistry.* 2011; 50:8323–8332. [PubMed: 21863786]
- [26]. Safo MK, Ahmed MH, Ghatge MS, Boyiri T. Hemoglobin-Ligand Binding: Understanding Hb Function and Allostery on Atomic Level. *Biochim. Biophys. Acta.* 2011; 1814:797–809. [PubMed: 21396487]
- [27]. Richard V, Dodson GG, Mauguen Y. Human Deoxyhaemoglobin-2,3-diphosphoglycerate Complex Low-Salt Structure at 2.5 Å Resolution. *J. Mol. Biol.* 1993; 233:270–274. [PubMed: 8377203]
- [28]. Vasquez GB, Ji X, Fronticelli C, Gilliland GL. Human Carboxyhemoglobin at 2.2 Å Resolution: Structure and Solvent Comparisons of R-state, R2-state and T-state Hemoglobins. *Acta Cryst.* 1998; D54:355–366.
- [29]. Yi J, Thomas LM, Richter-Addo GB. Crystal Structure of Human R-State Aquomethemoglobin at 2.0 Å Resolution. *Acta Cryst.* 2011; F 67:647–651.
- [30]. Silva MM, Rogers PH, Arnone A. A Third Quaternary Structure of Human Hemoglobin A at 1.7 Å Resolution. *J. Biol. Chem.* 1992; 267:17248–17256. [PubMed: 1512262]
- [31]. Safo MK, Abraham DJ. The Enigma of the Liganded Hemoglobin End State: A Novel Quaternary Structure of Human Carbonmonoxy Hemoglobin. *Biochemistry.* 2005; 44:8347–8359. [PubMed: 15938624]
- [32]. Petruk AA, Vergara A, Estrin D, Merlino A. Molecular Basis of the NO Trans Influence in Quaternary T-state Human Hemoglobin: A Computational Study. *FEBS Lett.* 2013; 587:2393–2398. [PubMed: 23770098]

**Highlights**

- The crystal structure of the NO derivative of *R*-state human Hb has been determined
- The Fe centers in both  $\alpha$  and  $\beta$  subunits are six-coordinate
- Structural differences in the FeNO moieties suggest a stronger interaction of NO with Fe in the  $\alpha$  subunit
- The hydrogen bonding patterns suggest a greater retention of NO in the  $\alpha$  distal pocket



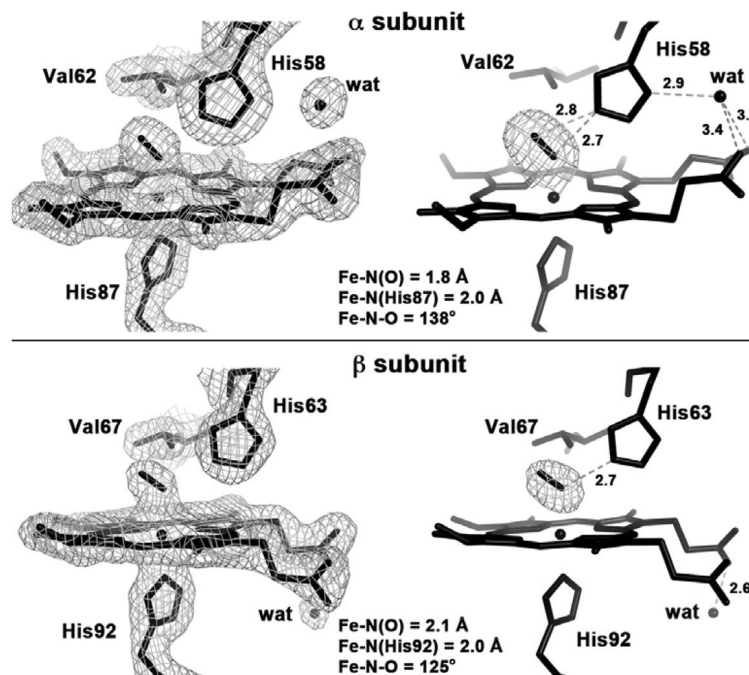


**Fig. 1.**

The  $2F_o - F_c$  omit electron density maps (left, contoured at  $1.0 \sigma$ ), the  $F_o - F_c$  omit electron density maps (right, contoured at  $3.0 \sigma$ ) and the final model of the heme active sites of the  $\alpha$  subunit (top) and  $\beta$  subunit (bottom) of *R*-state Hb(NO) (PDB access code: 4N8T, 1.9 Å resolution; this work).

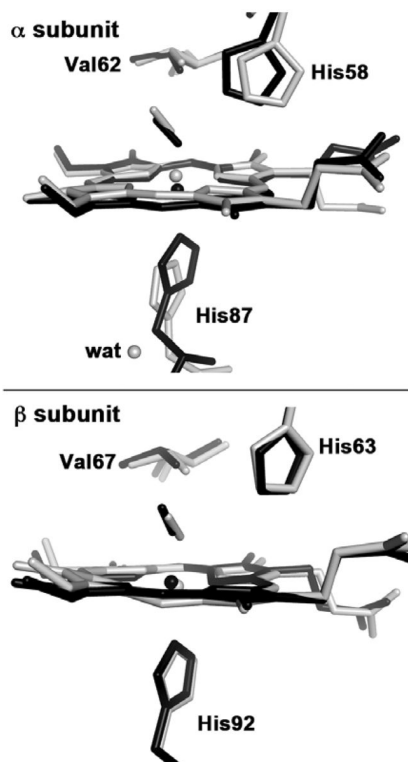


**Fig. 2.** Final models of the heme active sites of superimposed human *T*-state Hb(NO) (gray: PDB accession code 1RPS, 2.11 Å resolution)[14] and human *R*-state Hb(NO) (black; PDB accession code 4N8T, 1.9 Å resolution, this work), using the C $\alpha$ atoms of the protein backbone for the superposition.

**Table 1**Data Collection and Refinement Statistics<sup>a</sup>

PDB accession code	4N8T
Space Group	<i>P4<sub>1</sub>2<sub>1</sub>2</i>
Cell <i>a</i> , <i>b</i> , <i>c</i> (Å)	53.57, 53.57, 192.50
wavelength (Å)	1.0809
resolution range (Å)	24.5–1.90
no. of observations	280026
no. of unique reflections	23142
completeness (%)	100 (100)
<i>I</i> / $\sigma$ ( <i>I</i> )	17.9 (6.3)
<i>R</i> <sub>merge</sub>	0.071 (0.375)
<i>R</i> -factor	0.203
<i>R</i> <sub>free</sub> <sup>b</sup>	0.252

<sup>a</sup>The data in brackets refer to the highest resolution shell (1.97–1.90 Å).

<sup>b</sup>*R*<sub>free</sub> was calculated using 5% of the randomly selected diffraction data which were excluded from the refinement.